Journal of South American Earth Sciences 48 (2013) 73–84

Contents lists available at ScienceDirect

Journal of South American Earth Sciences

journal homepage: www.elsevier.com/locate/jsames

The E-MORB like geochemical features of the Early Paleozoic mafic-ultramafic belt of the Cuyania terrane, western Argentina

F.L. Boedo [a, *], G.I. Vujovich [a], S.M. Kay [b], J.P. Ariza [c], S.B. Pérez Luján [d]

[a] Instituto de Estudios Andinos Don Pablo Groeber (UBA-CONICET), Departamento de Ciencias Geológicas, Facultad de Ciencias Exactas y Naturales, Universidad de Buenos Aires, Buenos Aires, Argentina
[b] Cornell University, Department of Earth and Atmospheric Sciences and INSTOC, Ithaca, NY 14853, United States
[c] Instituto Geofísico Sismológico Ing. Volponi (UNSJ-CONICET), Facultad de Ciencias Exactas, Físicas y Naturales, Universidad Nacional de San Juan, San Juan, Argentina
[d] CONICET – Dpto. de Geofísica y Astronomía, Facultad de Ciencias Exactas, Físicas y Naturales, Universidad Nacional de San Juan, San Juan, Argentina

ARTICLE INFO

Article history:
Received 7 June 2013
Accepted 3 September 2013

Keywords:
Geochemistry
Western Precordillera
Continental margin ophiolite
Western Gondwana

ABSTRACT

The Argentine Precordillera is located in the central western region of Argentina, within the Central Andes. Throughout its westernmost sector, mafic and ultramafic bodies including serpentinites, mafic granulites, basaltic dikes/sills and pillow lavas are associated with metasedimentary rocks deposited in a deep marine and slope environment. These magmatic units, which are known as the Precordillera ultramafic-mafic belt, are considered to have a range of Early Paleozoic age based on published U–Pb zircon ages and fossil fauna. The entire sequence shows the effects of complex polyphase Paleozoic deformation and was subjected to a low grade metamorphism considered to be of middle-late Devonian age. The chemistry of the Peñasco and Cortaderas mafic dikes and sills in the southern part of this belt, which are largely plagioclase + clinopyroxene-bearing tholeiitic basalts, is the focus of this study. These volcanic rocks all have E-MORB-like major and trace element and εNd (+6.0 to +9.3) signatures with similarities to those previously reported throughout the belt. The new descriptions and major and trace-element analyses presented here confirm the similarity of the E-MORB-like chemistry of the Early Paleozoic mafic rocks along the entire belt, which spans some 500 km in length. There is a general consensus that these units are exposed as a consequence of the collision of the Chilenia terrane against the Gondwana margin during the middle to late Devonian, but the details of timing, the origins of the continental blocks and the nature of the collision are still debated. The results presented support the western Precordillera basaltic dikes/sills as having formed in the early stages of oceanic rifting along the Gondwana (Precordillera) continental margin with their E-MORB-like character reflecting mixing of depleted and enriched mantle and continental lithospheric sources.

1. Introduction

The basement of the South American plate, at the latitude of the Central Andes from 28°S to 33°S, consists of different terrains accreted to the Gondwana margin during the Paleozoic (e.g., Ramos et al., 1986). The boundaries between these terranes are evidenced by regional lineaments, mafic-ultramafic belts, presence of magmatic arcs associated with ancient subduction zones and other distinctive tectonic features. Particularly, the boundary between the Cuyania and Chilenia terranes (Fig. 1a) is marked by the presence of a mafic-ultramafic belt that outcrops in the western margin of the Argentine Precordillera.

The modern Argentine Precordillera (Fig. 1a) is located in west-central Argentina, over the subhorizontal segment of the subducting Nazca plate. It is part of the easternmost sector of the Andean orogenic front and can be divided into the eastern, central and western Precordillera based on its stratigraphic and structural characteristics (Baldis and Chebli, 1969; Ortiz and Zambrano, 1981; Baldis et al., 1982). The western and central parts of the Precordillera constitute a west-vergent thin-skinned belt, whereas the eastern Precordillera corresponds to an east-vergent basement block. The basement of the central Precordillera is indirectly known from xenoliths in Miocene volcanic rocks (Leveratto, 1968), which

* Corresponding author. Int. Güiraldes 2160 (1428), Departamento de Ciencias Geológicas, Facultad de Ciencias Exactas y Naturales, Universidad de Buenos Aires, Buenos Aires, Argentina. Tel.: +54 11 4576 3400x245.
E-mail addresses: florenciaboedo@gmail.com (F.L. Boedo), graciela@gl.fcen.uba.ar (G.I. Vujovich), smk16@cornell.edu (S.M. Kay), juampariza@yahoo.com.ar (J.P. Ariza), sofiap.lujan@unsj-cuim.edu.ar (S.B. Pérez Luján).

0895-9811/$ – see front matter © 2013 Elsevier Ltd. All rights reserved.
http://dx.doi.org/10.1016/j.jsames.2013.09.003

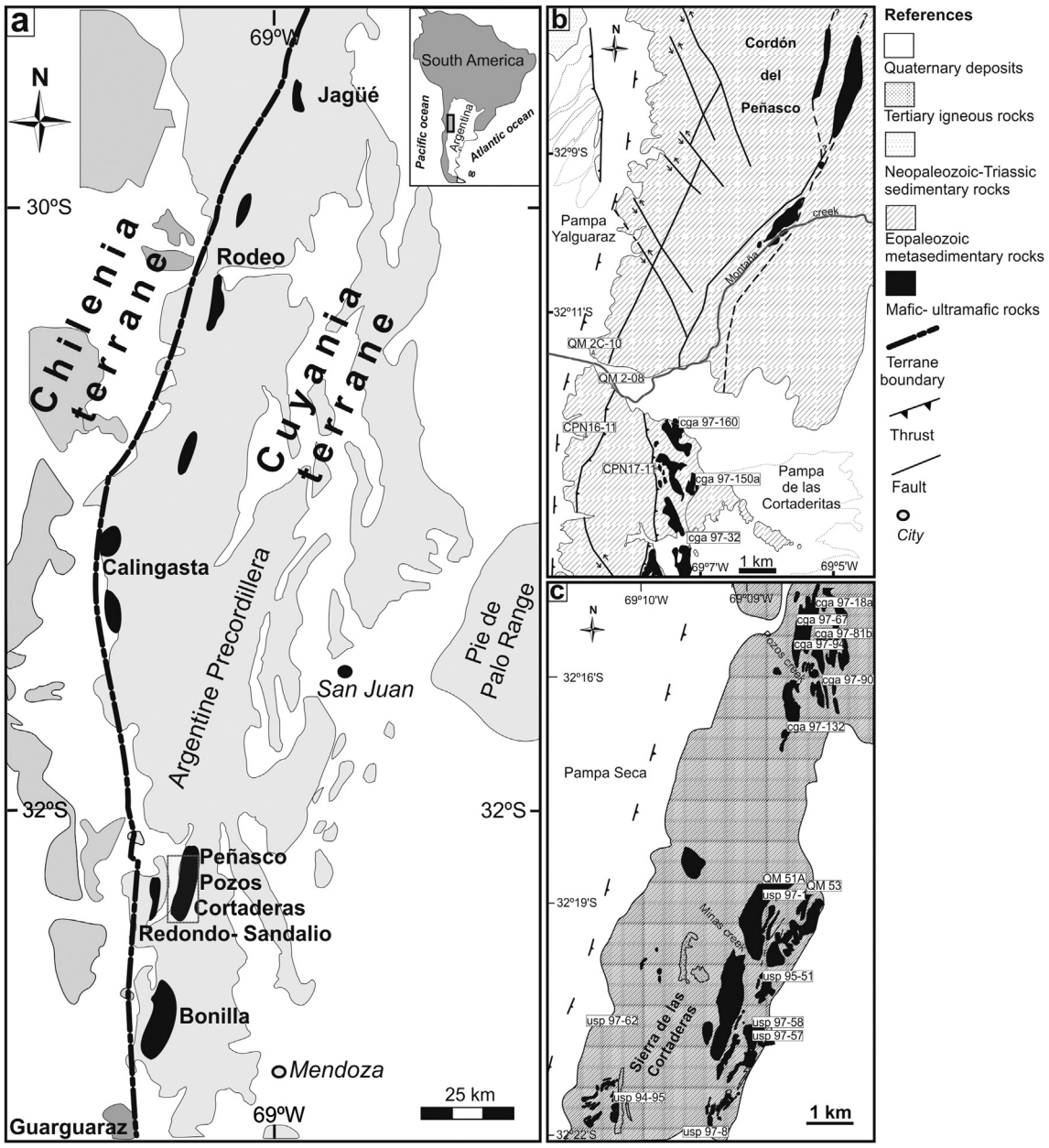

Fig. 1. a) Schematic geological map of central-western Argentina showing the boundary between the Cuyania (to the east) and Chilenia (to the west) terranes. This boundary is evidenced by the Precordillera mafic-ultramafic belt. b) Geological map of the Peñasco area modified from Boedo et al. (2012). c) Geological map of the Cortaderas area modified from Davis et al. (1999).

have yielded U/Pb zircon ages near 1100 My (Kay et al., 1996; Rapela et al., 2010). Distinctive Early Paleozoic stratigraphic sequences are well documented in the three subunits of the Precordillera. Particularly, the western Precordillera consists of slope and deep marine siliciclastic facies, some of which include carbonate platform and basement siliciclastic olistoliths (Thomas and Astini, 2003 and others therein). These associations are spatially related with mafic and ultramafic bodies, which are grouped into the Precordillera mafic-ultramafic belt. This belt extends discontinuously between 28°S and 33°S latitude and consists of pillow lavas, basaltic dikes and sills, massive gabbros, mafic granulites (layered gabbros) and serpentinized ultramafic rocks with E-MORB-like (*Enriched Mid-Ocean Ridge Basalts*) chemical signature and positive εNd values (+6 to +9.3) (Haller and Ramos, 1984, 1993; Kay et al., 1984; Ramos et al., 1986; Cortés and Kay, 1994; Davis et al., 2000; Fauqué and Villar, 2003; Kay et al., 2005). Both the meta-igneous bodies and the meta-sedimentary rocks record a greenschist facies metamorphic event, whose middle to late Devonian age is based on K–Ar and Ar–Ar mica ages (Cucchi, 1971; Buggisch et al., 1994; Davis et al., 1999).

The Precordillera mafic-ultramafic belt can be divided into two regional sectors. The first includes the Jagüé, Rodeo and Calingasta localities in the central and northern part of the belt (Fig. 1a). The mafic and ultramafic units in this region consist principally of pillow lavas, basaltic dikes and sills and massive gabbros. These units are interlayered or in tectonic contact with deep-marine metasediments which have been assigned Ordovician ages based on graptolite faunas (Blasco and Ramos, 1976; Brussa, 1999) and a zircon U–Pb age of 454 ± 35 My (Fauqué and Villar, 2003). Both the mafic and meta-sedimentary rocks have been affected by a low

Table 1
Chemical data set of the Cortaderas and Peñasco mafic dikes and sills. Major and trace element contents are given in wt% and ppm, respectively.

	usp97-1	usp94-51	usp97-58	cga97-67	cga97-81b	usp97-8	usp97-57	usp95-62	cga97-18a	cga97-90	cga97-94	cga97-132a	usp94-95	QM 51A	QM 53	cga97-150a	cga97-32	cga97-160	QM 2-08	QM 2C-10	CPN 16-11	CPN 17-11
SiO_2	50.71	49.33	49.30	49.35	47.98	48.38	49.81	42.79	49.77	48.00	48.96	49.22	48.65	48.17	45.95	49.50	50.60	48.36	46.04	45.29	47.33	47.6
TiO_2	2.26	1.58	1.82	1.91	1.33	2.96	1.98	0.88	2.01	1.42	2.47	2.09	1.98	1.75	2.12	2.30	2.09	2.35	1.32	1.58	2.13	1.37
Al_2O_3	15.23	13.95	14.04	13.74	18.14	13.28	14.37	15.31	14.59	14.87	14.22	14.01	17.91	14.47	14.59	13.70	15.01	14.20	16.97	15.86	13.84	13.2
FeO	12.73	11.60	12.15	11.79	10.83	14.99	12.26	10.34	11.73	11.29	13.43	12.45	10.77	10.09	10.59	12.83	11.77	14.19	13.15	16.70	17.78	14.5
MnO	0.20	0.18	0.24	0.23	0.21	0.22	0.17	0.18	0.20	0.17	0.24	0.20	0.15	0.19	0.20	0.20	0.20	0.22	0.15	0.19	0.21	0.2
MgO	5.36	8.59	7.32	7.42	5.42	6.64	6.41	14.30	6.00	7.94	6.19	7.55	5.03	5.87	6.52	6.37	5.53	5.68	7.13	7.15	6.35	8.2
CaO	7.90	12.52	11.87	12.03	12.57	9.25	11.20	16.24	11.21	13.75	11.60	11.20	11.17	10.67	10.83	10.83	10.95	12.05	12.55	10.11	10.21	13.0
Na_2O	3.42	2.16	2.23	2.98	2.43	3.32	2.42	0.18	2.90	2.14	2.12	2.71	2.79	2.42	2.38	2.80	2.74	1.71	2.03	2.74	2.61	2.0
K_2O	0.52	0.15	0.28	0.35	0.20	0.20	0.50	0.02	0.38	0.20	0.09	0.52	0.62	0.21	0.26	0.77	0.51	0.10	1.00	0.06	0.17	0.2
P_20_5	0.36	0.29	0.29	0.33	0.27	0.42	0.33	0.25	0.35	0.28	0.34	0.29	0.34	0.16	0.20	0.32	0.37	0.47	0.12	0.13	0.19	0.1
LOI	0.02	0.04	0.03	0.05	0.02	0.02	0.05	0.10	0.02	0.06	0.02	0.05	0.04	3.41	4.06	0.01	0.03	0.02	3.41	3.63	3.39	3.3
Total	98.69	100.35	99.54	100.13	99.38	99.66	99.45	100.59	99.16	100.12	99.68	100.29	99.45	97.41	97.69	99.62	99.80	99.35	101.00	99.72	100.30	100.5
La	8.42	5.77	6.43	8.18	6.45	16.28	8.75	4.59	8.83	4.78	10.94	7.65	9.83	8.3	12.8	10.43	9.68	11.42	5.60	4.90	8.90	5.30
Ce	23.5	16.6	17.3	20.9	17.2	40.6	23.5	13.8	23.3	14.0	27.2	20.6	31.3	19.9	27.7	25.9	24.5	28.9	14.6	12.8	23.8	14.3
Pr	–	–	–	–	–	–	–	–	–	–	–	–	–	2.8	4.1	–	–	–	1.94	1.76	3.17	1.91
Nd	17.0	12.6	14.4	11.9	13.7	26.3	16.8	9.30	14.9	8.18	16.6	15.8	19.0	13.2	19.0	15.6	17.7	18.7	9.50	8.80	15.4	9.70
Pm	–	–	–	–	–	–	–	–	–	–	–	–	–	–	–	–	–	–	–	–	–	–
Sm	4.92	3.77	3.91	4.32	3.71	6.90	4.77	2.30	4.65	2.94	5.48	4.24	5.08	3.9	5.6	5.27	4.98	5.77	2.60	2.80	4.50	2.90
Eu	1.71	1.28	1.32	1.48	1.39	2.23	1.56	0.98	1.54	1.08	1.88	1.38	1.65	1.4	1.7	1.87	1.68	2.05	1.08	1.13	1.62	1.20
Gd	–	–	–	–	–	–	–	–	–	–	–	–	–	4.7	5.6	–	–	–	3.20	3.60	5.60	3.70
Tb	1.16	0.80	0.88	0.90	0.83	1.57	1.15	0.59	1.00	0.71	1.17	0.84	0.91	0.8	1.0	1.19	1.03	1.25	0.60	0.60	0.90	0.60
Dy	–	–	–	–	–	–	–	–	–	–	–	–	–	5.3	6.1	–	–	–	3.50	3.90	5.90	3.70
Ho	–	–	–	–	–	–	–	–	–	–	–	–	–	1.1	1.2	–	–	–	0.70	0.80	1.20	0.70
Er	–	–	–	–	–	–	–	–	–	–	–	–	–	3.0	3.4	–	–	–	2.00	2.30	3.30	2.10
Tm	–	–	–	–	–	–	–	–	–	–	–	–	–	0.4	0.5	–	–	–	0.28	0.32	0.48	0.30
Yb	3.62	2.69	2.82	3.02	2.40	4.31	3.21	2.68	3.14	2.26	3.40	2.91	2.54	2.7	3.0	3.35	3.16	3.98	1.80	2.10	3.10	2.00
Lu	0.49	0.39	0.40	0.41	0.38	0.58	0.44	0.40	0.45	0.32	0.52	0.41	0.34	0.4	0.4	0.49	0.47	0.54	0.28	0.33	0.47	0.32
Y	–	–	–	–	–	–	–	–	–	–	–	–	–	30.4	25.8	–	–	–	18	21	29	20
Sr	196	321	230	282	286	380	261	764	294	256	607	647	382	255	271	291	284	293	477	769	695	253
Ba	390	50	52	124	84	145	134	–	132	96	206	162	110	133	104	149	93	73	436	83	91	112
Cs	2.31	0.77	0.79	0.39	0.22	0.34	0.52	0.08	0.26	0.21	0.07	0.38	1.82	0.5	0.1	0.92	0.35	72.26	0.80	b.d.l	b.d.l	b.d.l
Rb	–	–	–	–	–	–	–	–	–	–	–	–	–	6.0	5.0	–	–	–	24	b.d.l	5	4
U	0.38	0.09	0.14	0.19	0.18	0.38	0.34	0.07	0.15	0.04	0.94	0.11	0.25	0.4	0.3	0.19	0.10	0.26	0.20	0.10	0.20	0.20
Th	0.62	0.41	0.48	0.53	0.51	1.36	0.69	0.56	0.64	0.38	0.85	0.67	0.97	0.6	1.3	0.87	0.85	0.95	0.50	0.40	0.90	0.50
Pb	–	–	–	–	–	–	–	–	–	–	–	–	–	b.d.l	b.d.l	–	–	–	b.d.l	b.d.l	b.d.l	b.d.l
Zr	–	–	–	–	–	–	–	–	–	–	–	–	–	127	93	–	–	–	73	73	126	76
Hf	3.57	2.44	2.81	3.29	2.77	5.43	3.63	1.54	3.53	2.06	4.44	3.12	3.69	2.6	3.3	4.08	3.88	4.55	1.90	1.90	3.10	1.90
Nb	–	–	–	–	–	–	–	–	–	–	–	–	–	8.1	6.3	–	–	–	5.0	4.0	9.0	5.0
Ta	0.63	0.44	0.48	0.54	0.45	1.20	0.59	0.27	0.63	0.33	0.72	0.44	0.72	0.5	0.6	0.69	0.72	0.76	0.40	0.30	0.60	0.40
Sc	46	51	47	49	39	48	45	47	45	49	46	43	28	39	44	45	41	44	35	47	43	46
Cr	32	362	133	239	54	124	167	586	156	290	130	306	105	90	200	123	106	88	360	220	180	400
Ni	51	119	84	69	58	77	68	397	55	102	45	85	69	80	90	52	48	46	130	70	70	140
Co	51	56	53	49	44	57	46	67	43	54	46	54	40	45	45	47	43	49	39	48	47	45

b.d.l: below detection limit.

grade metamorphic event. Rubinstein et al. (1998) carried out thermometry studies on the Calingasta pillow lavas and dikes and suggested they achieved temperatures between 239° and 304 °C. Robinson et al. (2005) estimated pressure and temperature (PT) conditions of 0.2–0.3 GPa and 200–350 °C for the mafic metaigneous units near Rodeo and Calingasta.

The southern sector includes the Peñasco, Cerro Redondo, Cortaderas, Bonilla and, possibly, the Guarguaraz localities (Fig. 1a). The units in this region consist of serpentinized ultramafic bodies, mafic granulites (layered gabbros), massive gabbros, pillow lavas, basaltic dikes, sills and metahyaloclastic rocks, which are now in the greenschist facies. Initial pressure and temperature conditions estimated by Davis et al. (1999) on the mafic granulites are 850–1000 °C at pressures of >0.9 GPa. These values are consistent with those estimated by Boedo et al. (2012) in the Peñasco area ($P > 0.9$ GPa, $T \approx 884$ °C). In the Guarguaraz area, Willner et al. (2011) estimated that the metabasalts and metasediments reached pressures of 1.2–1.4 GPa and temperatures of 470–530 °C. On the basis of mineralogical and textural aspects, the subsequent lower metamorphic temperature would not have been over 350 °C. The presence of phengite suggests high pressure conditions.

The vergence of the Early Paleozoic deformational features is still debated. Some authors postulate a top to the west vergence of the structures (Ramos et al., 1986, 1984; Cortés et al., 1999; von Gosen, 1997) whereas others propose a top to the east vergence based on the analysis of kinematic indicators (Davis et al., 1999; Gerbi et al., 2002).

The mafic-ultramafic belt has been suggested to represent an ophiolitic section formed in a mid-ocean ridge, obducted by the collision of the Chilenia terrane against the Gondwana margin in the middle-late Devonian (Haller and Ramos, 1984; Ramos et al., 1986, 1984). Kay et al. (1984) suggested the belt may have formed in the initial stages of opening of an oceanic basin. On the basis of U–Pb ages and geochemical data, Davis et al. (2000, 1999) proposed that the mafic and ultramafic bodies formed in several events in a combination of tectonic environments involving mid-ocean ridges and that the mafic granulites represent the roots of a magmatic arc formed above a west-dipping subduction zone. In an earlier interpretation based on the detrital and geochemical features of the sedimentary rocks, Loeske (1993) postulated that the mafic-ultramafic belt formed in the floor of a back-arc basin.

Understanding the petrological aspects of these mafic and ultramafic rocks is critical to determining the nature and history of the Paleozoic orogens in the region. For this reason, this contribution is aimed at adding to the understanding of the petrology and geochemistry of the mafic bodies of the western Argentine Precordillera. We compare the analyses presented here with those from similar bodies elsewhere in the western Precordillera with the goal of characterizing the entire mafic-ultramafic belt, correlating the various units and analyzing the tectonic environments.

2. Materials and methods

The samples studied here are mafic rocks from the Precordillera mafic-ultramafic belt in the Peñasco and Cortaderas localities (Fig. 1b–c). Those in the Peñasco locality are from the western part of the Quebrada de Montaña (Fig. 1b), and those from the Cortaderas locality are from the Quebrada de los Pozos area (Fig. 1c), the Quebrada de las Minas and the southern sector of the range (Fig. 1c).

The samples were prepared and analyzed following standard procedures. Special efforts were made to avoid portions containing veins of secondary minerals. Major and trace elements were analyzed for fifteen samples of the mafic dikes, sills and flows from the Cortaderas localities and seven mafic dikes and sills from the Peñasco locality (Table 1). Seven analyses from the Calingasta area (Quebrada del Salto) are included in Table 2 to provide a picture of the northern sector of the belt.

The Peñasco samples were analyzed at the ACTLABS Laboratories (Canada) using a lithium metaborate/tetraborate fusion procedure with measurements done by ICP-MS (coupled plasma mass spectrometer). The major element concentrations of the Cortaderas samples are from the University of California at Davis PhD thesis of Davis (1997) and were analyzed with a Cameca SX-50 electron microprobe analyzing glasses fused from powders of the samples. Beam conditions were 15 kV, 10 nA and 15 μ scanning beam width. The trace element analyses of these samples and all others not done at ACTLABS were performed at Cornell University using instrumental neutron activation analysis (INAA). See Kay et al. (1987) for a complete description of the INAA analytical techniques. The data are plotted on multielement, rare earth element (REE) and ternary diagrams in the figures in this paper. Normalization values are from the chondrite CI analyses in Sun and McDonough (1989) and from the Pyrolite Mantle analyses in McDonough and Sun (1995). The Eu anomalies (Eu/Eu*) are based on the equation $Eu^* = Eu_N/(Sm_N \times Gd_N)$ (e.g., Taylor and McLennan, 1985).

In order to make a general chemical characterization of the entire Precordillera mafic-ultramafic belt, we compared analyses with those from the Jagüé, Rodeo, Calingasta and Cerro Redondo localities, whose geochemical analyses are from Kay et al. (1984), Ramos et al. (1986), Cortés and Kay (1994), Fauqué and Villar (2003), González Menéndez et al. (2013) and unpublished data from the Calingasta Quebrada del Salto region in Table 2.

3. Results

3.1. Mafic rocks from the Peñasco and Cortaderas localities

The Peñasco and Cortaderas study areas are located in the northern part of Mendoza province between 32° 6′S and 32° 22′S

Table 2
Major and trace elements of the Calingasta mafic rocks (Quebrada del Salto region). Major and trace element contents are given in wt% and ppm respectively.

Sample	KMES1	KMES3	KMES4	KMES5	KMES9	KMES10	KMES11
SiO_2	50.51	49.96	48.55	50.50	48.08	50.62	48.45
TiO_2	2.48	2.04	1.99	2.25	1.84	1.23	1.34
Al_2O_3	14.10	17.39	17.11	14.73	15.24	15.06	17.44
FeO	11.46	10.43	10.31	12.13	12.38	11.48	10.06
MnO	0.20	0.18	0.18	0.22	0.20	0.22	0.16
MgO	6.05	4.86	5.68	5.94	7.84	7.49	7.58
CaO	10.90	11.89	11.92	10.57	10.67	8.85	12.36
Na_2O	2.55	2.41	3.50	2.40	3.75	4.03	1.96
K_2O	0.76	0.13	0.24	0.17	0.03	0.08	0.20
P_2O_5	0.41	0.02	0.12	0.23	0.07	0.45	0.11
Total	99.42	99.32	99.59	99.15	100.09	99.51	99.67
La	12.6	8.84	8.30	16.4	6.59	6.64	6.24
Ce	29.7	21.5	19.9	39.0	14.5	14.6	16.2
Nd	19.3	13.6	11.4	24.0	5.90	6.70	10.1
Pm	–	–	–	–	–	–	–
Sm	5.61	4.14	3.61	6.73	2.56	2.68	3.03
Eu	1.73	1.35	1.23	1.90	0.95	0.97	1.09
Tb	1.02	0.81	0.73	1.37	0.70	0.65	0.60
Yb	3.06	2.29	1.99	4.23	2.58	2.74	1.81
Lu	0.400	0.309	0.272	0.590	0.364	0.379	0.224
Sr	271	292	540	204	144	301	362
Ba	103	158	222	38	44	111	266
Cs	0.50	0.52	0.97	0.18	0.61	0.61	0.77
U	0.2	0.1	0.0	0.5	0.0	0.4	0.3
Th	0.89	0.64	0.61	1.24	0.50	0.47	0.43
Hf	4.7	3.2	2.7	5.5	2.0	2.1	2.3
Ta	0.88	0.64	0.63	1.20	0.40	0.55	0.47
Sc	41.9	31.7	35.0	43.3	51.2	44.1	32.4
Cr	73	85	152	147	238	208	282
Ni	63	59	67	58	71	76	141
Co	42	40	40	51	56	52	51

and 69° 4′W and 69° 10′W, and include the Cordón del Peñasco in the northern part (Fig. 1b), the Pozos area in the central part and the Sierra de Cortaderas in the southern part (Fig. 1c). The mafic dikes and sills, amygdaloidal massive flow units and less common metahyaloclastites in this region are spatially associated with slope and deep marine metasediments. Large bodies of highly serpentinized ultramafic rocks and retrograded mafic granulites (layered gabbros) are also present (Boedo et al., 2012). All of these successions are affected by greenschist facies metamorphism.

The mafic dikes and sills from the Peñasco and Cortaderas areas vary from meters to tens of meters in thickness. Where contacts are exposed, these dikes and sills are seen to intrude metasedimentary rocks (Fig. 2a). In hand specimen, the samples are dark green in color. They all have porphyritic to fine-grained textures, with white subhedral (plagioclase) and dark green to black anhedral mafic crystals, whose sizes range from 1 to 3 mm (Fig. 2b–c). The thicker bodies show margin to core grain size variations. Under the microscope, primary assemblages can be seen to have been partially obliterated by greenschist facies metamorphism (Fig. 2d). Fine-grained, porphyritic to seriated textures with ophitic and/or subophitic arrays are recognized. They are mainly made up of partially uralitized clinopyroxene and totally saussuritized plagioclase crystals. Apatite and ilmenite occur as accessory phases with chlorite, white mica, albite, tremolite-actinolite, epidote and less commonly titanite and magnetite occurring as secondary minerals (Dias and Zanoni de Tonel, 1992, 1987; Davis et al., 1999; Boedo et al., 2012).

Mafic volcanic rocks, whose individual flow units are usually a meter thick, are interlayered in the meta-sandstones and metapelitic units as discussed by Davis et al. (1999). In hand specimen, the samples have vesicular to amygdaloidal porphyritic to aphanitic textures and are strongly altered and deformed. Under the microscope, they have porphyritic to aphyric textures in which the groundmass is totally altered to a fine aggregate of albite + chlorite + opaque minerals + epidote. Vesicles are filled with calcite and, in a lesser extent, with quartz. In a few samples, Davis et al. (1999) observed altered clinopyroxene phenocrysts and, rarely, orthopyroxene and olivine.

3.1.1. *Geochemical aspects of mafic dikes and sills from the Peñasco area*

The whole rock analyses show that the Peñasco samples have wt % SiO_2 concentration that vary over a small range (45.3–47.6 wt%) with wt% Al_2O_3 ranging from 13.2 to 17 wt% and CaO ranging from 10 to 13 wt% and Mg# varying from 30 to 40 (wt% MgO varying between 5.5 and 8.2%). Total alkali contents (wt% $Na_2O + K_2O$) do not exceed 3%. Wt% TiO_2 is relatively high (1.3–2.1%) and wt% MnO and P_2O_5 values are less than 0.2%. Loss on ignition (LOI) values are about 3.4 wt%.

To classify these rocks, we have employed diagrams based on immobile elements including P_2O_5, Zr, Ti, Nb and Y. According to the Zr/Ti vs Nb/Y rock classification diagram of Winchester and Floyd (1977), the Peñasco samples are subalkaline basalts (Fig. 3a). Using the P_2O_5 vs Zr diagram (Winchester and Floyd, 1976) shown in Fig. 3b, the samples plot as subalkaline basalts and fall in the tholeiitic field, as do samples with similar lithologies from localities throughout the belt.

All of the Peñasco basaltic dikes and sills exhibit generally similar trace element patterns (Fig. 4a–b). Their features, as seen in

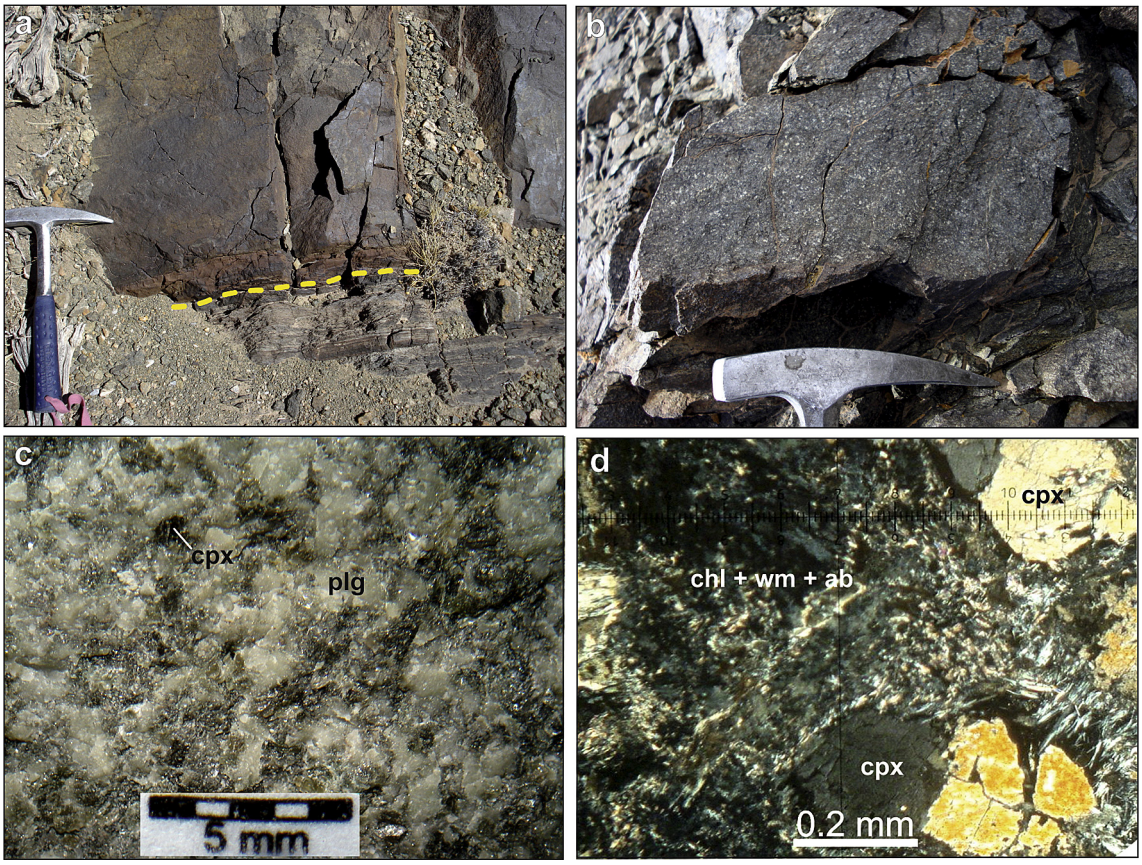

Fig. 2. a) The Peñasco area. Intrusive contact (dotted line) between a basaltic sill and phyllites with sedimentary protoliths. b) Fine to medium-grained basaltic sill. c) Medium-grained basaltic sill with white plagioclase and dark green to black clinopyroxene crystals. d) Basaltic dike under the microscope where relic clinopyroxene is distinguished among a fine-grained matrix of chlorite (chl), albite (ab) and white mica (wm).

Fig. 4a, include gently sloping REE patterns with a slight enrichment in light rare earth elements (LREE) over heavy rare earth elements (HREE). REE concentrations are 10–40 times higher than the chondritic values. The concentrations of elements such as Cs, Rb, Ba and K are erratic due to their mobility during alteration. Some samples show positive Sr anomalies, which can be related to the presence of plagioclase (Fig. 4b).

In detail, La/Yb ratios vary between 2.3 and 3.1, and fall within the range of values commonly occurring in mid-ocean ridge volcanic rocks (e.g., Moyen, 2009; Gale et al., 2013). La/Sm ratios range from 1.8 to 2.2 and Sm/Yb from 1.3 to 1.5. La/Ta ratios (13.3–16.3) are close to the values expected in MORB rocks, excluding a possible environment of formation in an arc/backarc setting, where La/Ta ratios should be greater than around 25 (e.g., Gale et al., 2013). Th/U ratios (2.5–8.7) are close to E-MORB values (e.g., Gale et al., 2013) and their scatter could be related to mobilization of U during secondary processes. Zr/Y ratios (3.5–4.3) suggest little continental crustal contamination (e.g., Bohlar et al., 2003). The samples also show low to moderate Sc (35–47 ppm), Ni (46–140 ppm) and Cr (180–400 ppm) concentrations.

3.1.2. *Geochemical aspects of mafic dikes, sills and volcanics from the Cortaderas area*

The major and trace element patterns of the mafic rocks from the Cortaderas area are similar to those of the Peñasco area samples (Fig. 5a–b). As in the Peñasco area samples, Mg# are from 30 to 60, with wt% MgO ranging from 5 to 14%, wt% Al_2O_3 from 13.3 to 18.1% and wt% TiO_2 up to 3%. Wt% CaO ranges between 7 and 17% and total alkali concentrations rarely exceed 4 wt%. Cs, Rb, Ba, U and K concentrations are erratic as a consequence of their mobility during alteration processes (Fig. 5b).

As with the Peñasco area samples, LREE are also slightly enriched over HREE in the Cortaderas area samples (Fig. 5a). Their La/Yb ratios range from 1.7 to 3.9, their La/Sm ratios are from 1.6 to 2.4 and their Sm/Yb ratios are 1.4–1.6, except in the two cases where Sm/Yb ratios are 0.9 and 2.0. Overall REE concentrations are between 10 and 45 times higher than those in chondrite CI. As in the Peñasco area samples, La/Ta ratios (13.6–16.8) are below those in arc and back-arc rocks and Th/U ratios (0.9–8.2, average: 3.9) are close to E-MORB values (e.g., Gale et al., 2013). The Cortaderas area samples also have concentrations of Cr from 31 to 585 ppm, of Sc between 27 and 51 ppm and of Ni from 46 to 396 ppm.

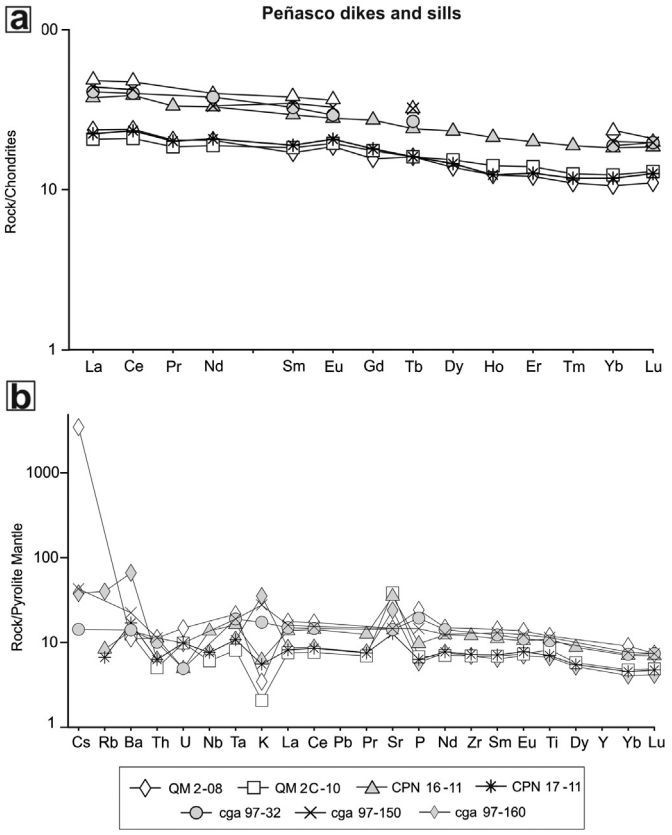

Fig. 4. a) Chondrite normalized REE diagram for the Peñasco samples. b) Pyrolite mantle normalized trace element diagram. The Peñasco dikes and sills patterns are shown.

3.2. *Geochemical aspects of mafic rocks from other areas of the Precordillera mafic-ultramafic belt and comparison with study areas*

3.2.1. *Mafic dikes, sills and flows from the northern sector (Jagüé, Rodeo, Calingasta)*

The northern part of the Precordillera mafic-ultramafic belt is mainly composed of mafic pillow lavas, dikes, sills and gabbros in the greenschist facies, which are interlayered or in tectonic contact

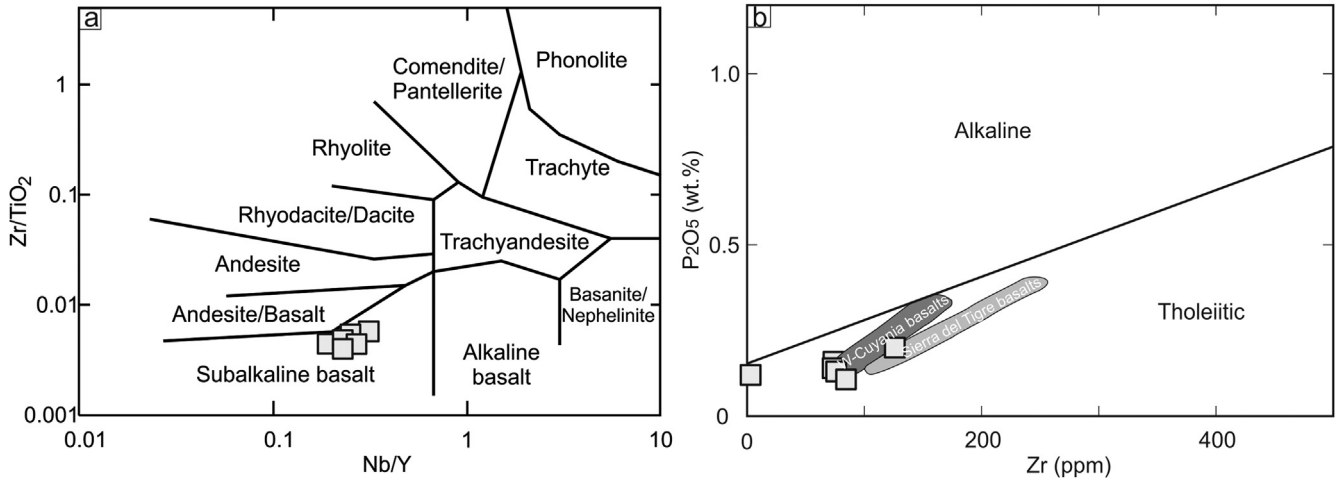

Fig. 3. a) Zr/TiO_2 vs Nb/Y classification diagram (Winchester and Floyd, 1977). Mafic rocks of the Peñasco area are subalkaline basalts. b) P_2O_5 vs Zr diagram for basalt classification (Winchester and Floyd, 1976). Basaltic dikes and sills from the Peñasco and Cortaderas areas are tholeiitic basalts.

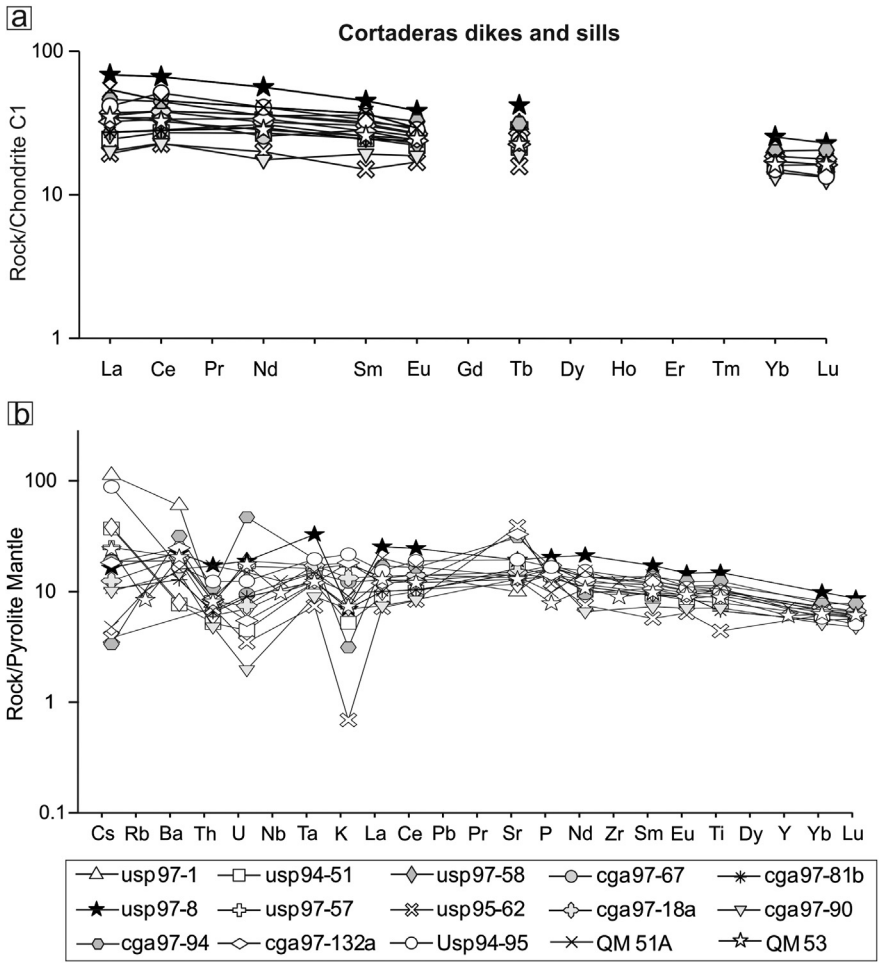

Fig. 5. a) Chondrite normalized REE diagram for the Cortaderas samples. b) Pyrolite mantle normalized extended trace element diagram. Dikes and sills patterns from the Cortaderas area are shown.

with Early Paleozoic metasediments. The rocks in the various regions are described below.

As described by Fauqué and Villar (2003), the pillow lavas at Jagüé (Fig. 1a) exhibit porphyritic to seriate textures and contain olivine, clinopyroxene and plagioclase phenocrysts. Their margins show hypocrystalline textures with fluidal structures. Under the microscope, the lavas show aphyric, intersertal or vitric textures and have plagioclase microliths, clinopyroxene phenocrysts and spinel xenocrystals.

Samples from dikes and sills in the Rodeo area (Fig. 1a) have porphyritic textures and contain calcic plagioclase and pyroxene phenocrysts. They are strongly propylitized and serpentinized with argilitized and carbonatized plagioclases and chloritized mafic minerals (Cardó and Diaz, 1999). In the Cuesta del Viento area, Haller and Ramos (1984) and Kay et al. (1984) described a sequence of ultramafic (wehrlite) dikes, pillow lavas and sills with columnar jointing. The wehrlites have cumulate textures with serpentinized olivine, clinopyroxene, chromite and titanomagnetite, and contain secondary talc and titanite (Kay et al., 1984; Cardó and Diaz, 1999). Cardó and Diaz (1999) also described spessartites with aphanitic texture composed of augite, serpentines, tremolite-actinolite, biotite and opaque minerals.

In the Sierra del Tigre, Haller and Ramos (1984) and González Menéndez et al. (2013) describe massive basalts and pillow lavas in tectonic contact with metapelites. These authors also mention basaltic sills intruding metasediments and massive coarse-grained gabbros that are in turn intruded by basaltic dikes.

The Calingasta mafic units (Fig. 1a) consist on basaltic dikes, sills and pillow lavas that contain olivine, clinopyroxene, plagioclase and opaque oxide phenocrysts. The basalts have porphyritic to seriate textures, with ophitic, subophitic, microgranular and intersertal aspects. Ilmenite and rutile occur as secondary minerals as do albite, chlorite, carbonate, titanite, leucoxene, amphibole, biotite, opaque minerals, quartz and zoisite (Quartino et al., 1971). Pyrite-pyrrhotite mineralization is superimposed (Quartino et al., 1971).

The major and trace element contents of the mafic rocks in the northern part of the belt (Kay et al., 1984; Fauqué and Villar, 2003; González Menéndez et al., 2013; this paper) are similar to those of the mafic dikes, sills and lava flows from the south, which are described above. Their wt% SiO_2 concentrations are between 45 and 51%, with Mg#s from 30 to 50 and wt% TiO_2 concentrations from 1.2 to 3.7%. Concentrations of wt% CaO range from 8.8% to 14.2%, wt% Al_2O_3 varies between 12% and 18% and wt% K_2O does not exceed 1%. High wt% Na_2O concentrations, which in some cases reach 4%, could be related to albitization.

Overall, their REE patterns are similar to those of the dikes, sills and flows from the south discussed above (Fig. 6a–c). As in those samples, their REEs are enriched, with concentrations that are 5–45 times higher than in CI chondrites, and their LREEs are enriched

relative to their HREEs. Their La/Sm ratios vary between 1.7 and 3.8. La/Yb ratios, which range from 2.4 to 4.2, can be slightly higher than those in samples to the south, but are still within the range found in E-MORB basalts (e.g., Moyen, 2009; Gale et al., 2013). The Jagüé samples (Fauqué and Villar, 2003) can have slightly positive Eu anomalies (Eu/Eu*: 1.0–1.2) which contrast with the Calingasta and Rodeo samples that can have mildly negative anomalies (0.8–0.9). Ppm Ba, Sr, U and Cs concentrations are variable due to mobility during alteration. Cr concentrations are 73–343 ppm, Sc concentrations are 31–52 ppm and Ni concentrations are less than 320 ppm.

3.2.2. *Mafic dikes, sills and flows from the southern sector (Cerro Redondo area)*

In the Cordón del Cerro Redondo and Cordón Sandalio area (Fig. 1a), pillow lavas of basaltic to andesitic-basaltic composition are intercalated in a metasedimentary succession (Cortés and Kay, 1994; Cortés et al., 1999).

Microscopically, these lavas have porphyritic textures with very fine intersertal, variolitic and ophitic groundmasses and up to a 10% of altered plagioclase phenocrysts. Besides, clinopyroxene, ilmenite and magnetite are recognized. Chlorite, epidote, calcite and serpentine occur as secondary phases (Cortés, 1992; Cortés and Kay, 1994; Cortés et al., 1999).

The rocks of this area also have major and trace element features similar to those of the samples described above. As in those samples, their REE patterns show relative enrichments of the LREEs over the HREEs, with REE concentrations between 9 and 30 times CI chondrite values (Fig. 6d). Ppm Cs, Sr, Ba, U concentrations are also variable, reflecting secondary processes.

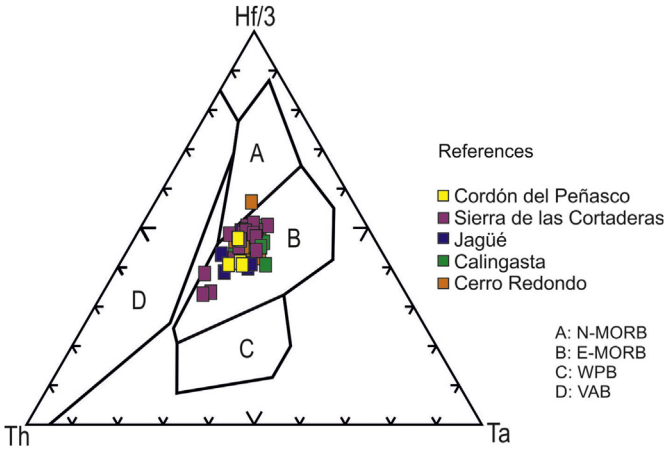

Fig. 7. Th–Hf/3-Ta tectonic discrimination diagram (Wood et al., 1979) where the basaltic dikes, sills and flows from the Precordillera mafic-ultramafic belt are plotted. The data fall within the E-MORB field and, to a minor extent, within the N-MORB field.

Cortés and Kay (1994) describe how minor Eu negative anomalies and low Ni concentrations indicate low pressure fractionation of plagioclase and olivine respectively, and that REE and Cr values are reflected by the presence of clinopyroxene. These authors suggest that the proportions of REE, Ta, Th and Hf indicate an oceanic source and note that the La/Ta ratios (13–15, similar to those of other localities) fall within the range of mid-ocean ridges and oceanic islands.

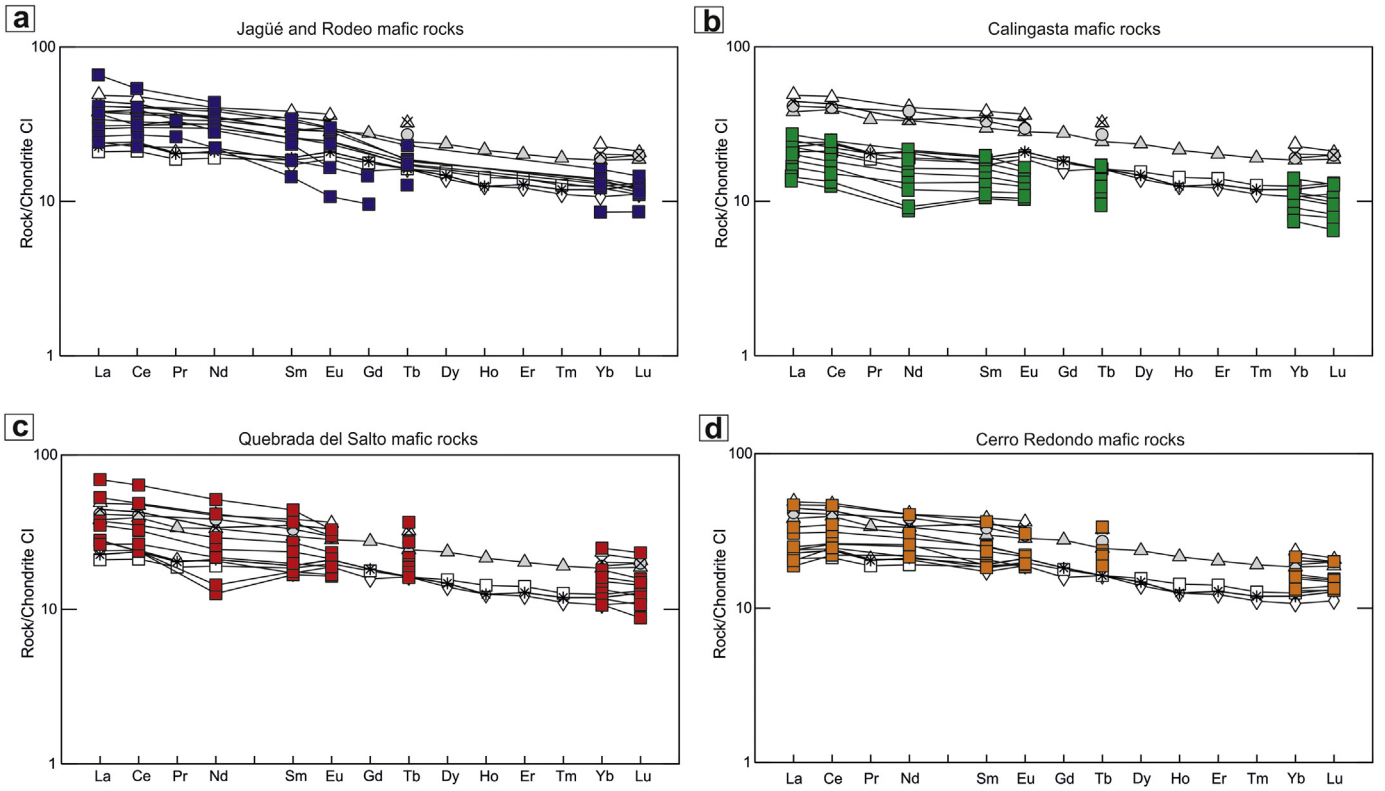

Fig. 6. a) Chondrite normalized REE diagram for samples from the northern part of the Precordillera mafic-ultramafic belt. Jagüé and Rodeo dikes and sills patterns are shown. b) Calingasta dikes and sills REE patterns. c) Quebrada del Salto dikes and sills REE patterns. Geochemical data from Kay et al. (1984), Fauqué and Villar (2003), González Menéndez et al. (2013) and this contribution. d) Chondrite normalized REE diagram for samples from the southern part of the Precordillera mafic-ultramafic belt. Dikes and sills patterns from the Cerro Redondo area are shown. Geochemical data from Cortés and Kay (1994). Peñasco samples are shown in all diagrams for comparison.

A plot of all of the samples discussed above on a Th–Hf/3-Ta ternary diagram (Wood et al., 1979) (Fig. 7) shows that they all fall within the field of intraplate oceanic basalts (E-MORB) field as is consistent with their REE patterns, La/Sm (1.6–3.8) and La/Yb (1.6–4.2) ratios falling within the typical ranges seen in E-MORB rocks. Considering these similarities, all of the tholeiitic basaltic rocks of the Precordillera mafic-ultramafic belt can have a generally similar tectonic setting.

4. Discussion

4.1. The E-MORB genesis debate

The origin of the E-MORB signature has been long discussed as it reflects different processes such as the composition of their source, the extent of mixing between different source components, the degree of melting and/or fractional crystallization, the tectonic environment, crustal contamination and alteration (e.g., Arevalo and McDonough, 2010). Overall, MORB type rocks are usually divided into normal-type MORB (N-MORB) and enriched-type MORB (E-MORB). The N-MORB signature is characterized by a relative depletion of highly incompatible compared to compatible elements, whereas the E-MORB signature has a component that is relatively enriched in incompatible elements, as seen by $(La/Sm)_N \geq 1$ as well as lower εNd and higher $^{87}Sr/^{86}Sr$ isotopic values (Arevalo and McDonough, 2010).

The E-MORB signature was originally proposed to result from an interaction between enriched mantle plumes and depleted mantle sources. However, lavas with E-MORB-like signatures have been found in mid-ocean ridges far from mantle plumes, in relative slow-spreading oceanic ridges and in wide backarc basins. As such, some E-MORBs are clearly associated with hotspots (Schilling, 1973; among others), whereas others are not clearly linked to any mantle plume and require a different explanation.

The concepts of mantle heterogeneity and metasomatism are widely used in discussing other ways to generate E-MORB-like signatures. In particular, recycling of oceanic lithosphere is considered an important mechanism in creating enriched heterogeneities within the mantle that can then generate rocks with an OIB (Oceanic Island Basalts) signature (White and Hofmann, 1982; Allègre et al., 1984; Allègre and Turcotte, 1986; Zindler and Hart, 1986; Sun and McDonough, 1989; among others). E-MORBs can then reflect the presence of OIB "diluted" material or depleted OIB material located in a sub-ridge mantle (Allègre and Turcotte, 1986; Zindler and Hart, 1986; among others). Enriched dikes and veins emplaced in depleted peridotite by metasomatism due to intrusion of low percentage melts provide another alternative to explain the enriched mantle component in E-MORB lavas (Niu et al., 2002; and others therein).

The genesis of these dikes and veins has been little discussed. Hèmond et al. (2006) discuss the two broad processes that can generate enriched sources: 1) recycling of alkali basalts found on oceanic islands and seamounts, or 2) recycling of subcontinental or suboceanic lithosphere enriched by metasomatism. Along these lines, Ulrich et al. (2012), among others, propose a binary mixture between N-MORB materials and OIB as being the origin of E-MORBs. Nevertheless, Niu et al. (2002) postulate that just recycling oceanic crust does not explain the high abundances of LILE and Th, U, Pb, etc. as when oceanic crust subducts and dehydrates, it becomes depleted in those elements. Instead, they argue that the deep parts of recycled oceanic lithosphere are important geochemical reservoirs of these and other incompatible elements as a result of metasomatism at the interface between the low-velocity zone (LVZ) and a cold and thick oceanic lithosphere. Enrichments in the incompatible trace elements (LREE, Th, U, Ti, Ta, Nb, among others) along with low MgO (~ 7%) are recognized along the Precordillera mafic-ultramafic belt and could be the result of small degrees of melting or great extents of fractional crystallization due to slow ridge spreading rates (Arevalo and McDonough, 2010).

According to Donelly et al. (2004), E-MORBs can be generated in two stages: 1) generation of low degree melts that infiltrate and metasomatize the upper mantle, 2) high degrees of partial melting of an already metasomatized mantle in a mid-ocean ridge environment. The two must be very separated in time to achieve the isotopic differences observed in N- and E-MORB lavas. In subduction zones, subducting oceanic crust is subjected to low degrees of partial melting, and the resulting melts metasomatize the overlying mantle wedge. Recycling by mantle convection makes metasomatized mantle undergo high degrees of partial melting and generates E-MORBs.

The E-MORB signature in the Early Paleozoic mafic dikes and sills studied here can be traced over 500 km along the Precordillera mafic-ultramafic belt. The similarities of their major and trace element geochemistry suggest that they have a common tectonomagmatic origin and that their mantle source composition reflects mixing of depleted and enriched mantle and continental lithospheric sources. The exact nature and origin of these components remains an area for future study in unraveling this issue.

4.2. The generation of mafic rocks from the Argentine Precordillera mafic-ultramafic belt

The tectonic environment of the Precordillera mafic-ultramafic belt has not been definitively determined. Nevertheless, there is some consensus that the belt represents an ophiolite or dismembered ophiolitic sequence, which has remained along the suture between the Chilenia and Gondwana (Cuyania) terranes (e.g., Haller and Ramos, 1984; Ramos et al., 1984, 1986). This collision is generally placed in middle to late Devonian times based on K/Ar and Ar/Ar white mica ages (Cucchi, 1971; Buggisch et al., 1994; Davis et al., 1999). Davis et al. (1999) used U/Pb zircon ages to go a step further and argue that the mafic-ultramafic belt is a composite of ophiolitic sequences emplaced in a series of events from the Neoproterozoic to the Devonian. In contrast, Loeske (1993) argued that the western margin of Gondwana varied from a passive to an active margin in Early Paleozoic times with the formation of a back-arc basin in this region based on detrital modes, geochemical and REE patterns of psammites and the presence of pillow basalts. The E-MORB signature and high Ba, Th and Nb values of the basalts were interpreted as reflecting their formation as nearly uncontaminated back-arc rift basalts. The models all agree in the passage from a passive to an active margin, with subduction of oceanic crust, but diverge in the polarity of the subduction zone and the tectonic details of the formation of the ultramafic and mafic rocks.

Based on geochemical data, Kay et al. (1984) proposed that the mafic rocks could not have originated in an island arc, but could have potentially formed in a broad back-arc basin or at a mid-ocean ridge with an enriched source or as an early oceanic rift next to a continental margin. The latter was their preferred model. More recently, González Menéndez et al. (2013) have again argued against the mafic rocks being related to subduction or either an N-MORB or OIB environment. According to their geochemical model, the Precordillera mafic rocks were derived from mantle sources with compositions similar to primordial mantle in the garnet-spinel transition zone. They propose that the belt largely formed on a thinned continental margin as mafic volcanism developed between the Chilenia and Cuyania terranes during the middle to late Ordovician. Their hypothesis in part supports models

proposing that the Chilenia and Cuyania terranes were part of a larger terrane called Occidentalia, which was either derived from southern Laurentia or was autochthonous to Gondwana (Dalla Salda et al., 1992; Dalziel et al., 1994; among others).

Both the field relations and geochemical features support the basaltic dikes and sills being associated with igneous activity typical of a growing oceanic basin. This is consistent with these basalts representing the early stage of a non-subduction related ophiolite or a Continental Margin Ophiolite according to the ophiolite classification of Dilek and Furnes (2011). Along the western margin of the Argentine Precordillera, many authors have observed evidence for an east–west extensional regime developing in a passive margin environment during the Ordovician (e.g., Alonso et al., 2008; and others therein). This evolution seems to have continued into the Silurian and possibly the early Devonian based on basaltic dikes, sills and lavas in Silurian-Devonian (age based on plant fossils) meta-sedimentary rocks (Cortés, 1992; Cortés and Kay, 1994) and an U/Pb age of 418 ± 10 My from a zircon in a mafic sill (Davis et al., 2000). In this context (Fig. 8), the body of water to the west could not have reached great depths in the Peñasco and Cortaderas areas as medium to fine-grained meta-sandstones, with thicknesses up to 2 m are dominant whereas pelitic deposits are scarce or almost nonexistent in some regions. Occasionally, amalgamated medium-grained meta-sandstones and thick coarse-grained meta-sandstones and fine conglomerates are recognized. The preserved sedimentary structures indicate turbiditic sedimentation in the proximal areas. Moreover, Boedo et al. (2012) describe vesicular and amygdaloidal metabasalts interlayered with meta-hyaloclastites, which are consistent with shallow water. These deposits have been assigned to the late Ordovician-early Devonian by Cortés et al. (1999) on the basis of regional stratigraphic relationships.

In accordance with the regional context and these field relations, the basaltic dikes and sills in the Precordillera could have intruded into a thinned continental margin or an oceanic–continental transition zone prior to or as a passive margin developed in the context of an incipient oceanic basin.

The several geotectonic models so far proposed by different authors have various advantages and disadvantages. Possible tectonic scenarios for the development of a tholeiitic basaltic magmatism with an E-MORB signature in a regional terrane model are:

1) Both the Chilenia and Cuyania terranes were allochthonous to Gondwana. The Cuyania terrane is of Laurentian origin (e.g., Thomas and Astini, 2003; Thomas et al., 2012), and collided against the Proto-Gondwana margin in the late Ordovician. During the middle-late Devonian, the Chilenia terrane, whose origin is still controversial, would have accreted against the Gondwana margin (Ramos et al., 1986).
2) The Chilenia and Cuyania terranes were part of a larger terrane (Occidentalia?) that accreted to Gondwana in the late Ordovician (Dalla Salda et al., 1992; Dalziel et al., 1994; among others). After the collision, the Chilenia terrane was separated from Cuyania forming a small ocean basin, which may have been wider to the south. At this stage, an extensional environment developed on the western margin of the Precordillera, where the mafic bodies formed. Finally, the development of a subduction zone (whose polarity is still debated) closed the oceanic basin and the Chilenia terrane collided against the Gondwana margin (Cuyania terrane) in the middle-late Devonian (Davis et al., 2000; González Menéndez et al., 2013). In this model, the Chilenia terrane is parautocthonous from Cuyania.
3) The Chilenia and Cuyania terranes rifted from Laurentia in the early Cambrian and collided against the Gondwana margin during the late Ordovician. A successful rift occurred west of Chilenia, whereas only a small oceanic basin developed between Chilena and Cuyania. It is noteworthy in this regard that the basements of the two terranes have distinct isotopic signatures (Kay et al., 1996).

5. Conclusions

We have presented new geochemical data from the southern sector of the Precordillera mafic-ultramafic belt and compared the geochemical analysis of the mafic rocks from the Peñasco and Cortaderas areas with similar lithological units in other parts of the Precordillera mafic-ultramafic belt. The main conclusions are:

- The mafic dikes and sills in the Peñasco and Cortaderas areas are tholeiitic basalts with E-MORB geochemical signature.
- Throughout the Precordillera, the volcanic rocks of the mafic-ultramafic belt are tholeiitic basalts with generally similar major and trace element signatures and phenocryst contents. Their trace element characteristics include LREE and wt% TiO_2 enrichments, restricted ranges of wt% SiO_2 and MgO, low N-MORB-like La/Yb ratios and a lack of high field strength element depletions. These similarities suggest a generally common tectonomagmatic origin.
- The basaltic dikes and sills are intruded into deep marine and slope environment sedimentary units and constitute part of a non-subduction-related ophiolite, which is classified as a Continental Margin Ophiolite. These basalts are best interpreted as

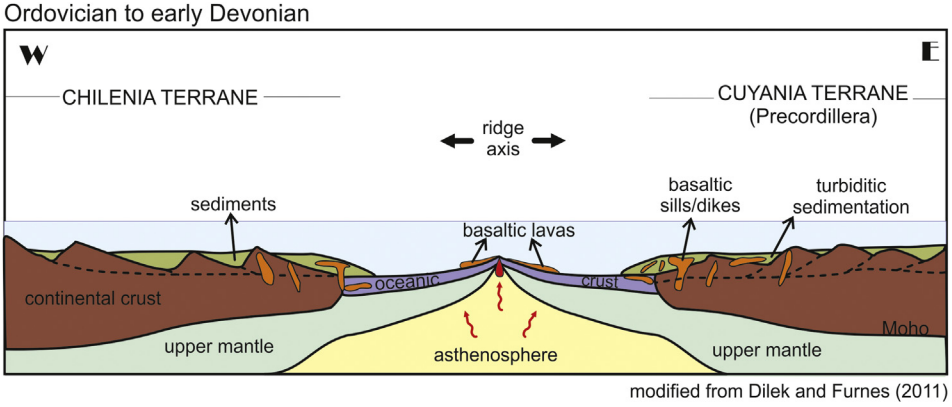

Fig. 8. Tectonic setting diagram for the basaltic dikes and sills from the western Precordillera mafic-ultramafic belt. During the Ordovician-Early Devonian, Cuyania was separated from the Chilenia terrane by a shallow oceanic basin. Decompressional partial melting was caused by rifting and basaltic E-MORB like dikes, sills and flows were generated.

having formed in an extensional environment on a thinned continental margin facing a shallow ocean basin.

Acknowledgments

This is the R-104 contribution of the Instituto de Estudios Andinos Don Pablo Groeber. This research has been developed within Florencia L. Boedo's PhD thesis and has been funded by research projects CONICET PIP 0072 and UBACyT 20020100100862 (Graciela Vujovich). We thank Harald Furnes and Alina Tibaldi for their constructive reviews.

References

Allègre, C.J., Hamelin, B., Dupré, B., 1984. Statistical analysis of isotopic ratios in MORB: the mantle blob cluster model and the convective regime of the mantle. Earth Planet Sci. Lett. 71, 71–84.

Allègre, C.J., Turcotte, D.L., 1986. Implications of a two-component marble-cake mantle. Nature 323, 123–127.

Alonso, J.L., Gallastegui, J., García-Sansegundo, J., Farias, P., Rodríguez Fernández, L.R., Ramos, V.A., 2008. Extensional tectonics and gravitational collapse in an Ordovician passive margin: the Western Argentine Precordillera. Gondwana Res. 13, 204–215.

Arevalo Jr., R., McDonough, W.F., 2010. Chemical variations and regional diversity observed in MORB. Chem. Geol. 271, 70–85.

Baldis, B., Chebli, G., 1969. Estructura profunda del área central de la Precordillera sanjuanina. In: 4° Jornadas Geológicas Argentinas, Actas 1, pp. 47–66.

Baldis, B., Beresi, M., Bordonaro, O., Vaca, A., 1982. Síntesis evolutiva de la Precordillera Argentina. In: 5° Congreso Latinoamericano de Geología, Actas 4, pp. 399–445.

Blasco, G., Ramos, V.A., 1976. Graptolitos caradocianos de la Formación Yerba Loca y del cerro La Chilca, Depto. Jáchal, Provincia de San Juan. Ameghiniana 13 (3/4), 312–329.

Boedo, F.L., Vujovich, G.I., Barredo, S.P., 2012. Caracterización de rocas ultramáficas, máficas y metasedimentarias del cordón del Peñasco, Precordillera occidental, Mendoza. Rev. Asoc. Geol. Argentina 69 (2), 275–285.

Bohlar, R., Woodhead, J.D., Hertg, J.M., 2003. Continental setting inferred for emplacement of the 2.9–2.7 Ga Belingwe Greenstone Belt, Zimbabwe. Geology 31 (4), 295–298.

Brussa, E.D., 1999. El género *Holmograptus* (Graptolithina) en el Ordovícico de la Precordillera occidental Argentina. Rev. Esp. Paleontol. 14, 183–190.

Buggisch, W., von Gosen, W., Henjes-Kunst, F., Krumm, S., 1994. The age of early Paleozoic deformation and metamorphism in the Argentine Precordillera-evidence from K-Ar data. Zentral. Geol. Paläontol. Teil I, 275–286.

Cardó, R., Diaz, I.N., 1999. Hoja Geológica 3169-01 Rodeo, San Juan (Informe Preliminar). Carta Geológica de la República Argentina, Servicio Geológico Minero Argentino. Escala 1:250.000.

Cortés, J.M., 1992. Lavas almohadilladas en el Grupo Ciénaga del Medio del extremo noroccidental de la Precordillera mendocina. Rev. Asoc. Geol. Argentina 47 (1), 115–117.

Cortés, J.M., Kay, S.M., 1994. Una dorsal oceánica como origen de las lavas almohadilladas del Grupo Ciénaga del Medio (Silúrico-Devónico) de la Precordillera de Mendoza, Argentina. In: 7° Congreso Geológico Chileno, Actas 2, pp. 1005–1009.

Cortés, J.M., González Bonorino, G., Koukharsky, M.L., Brodtkorb, A., Pereyra, F., 1999. Hoja Geológica 3369-03 Yalguaraz, Mendoza (versión preliminar), Carta Geológica de la República Argentina, Servicio Geológico Minero Argentino. Escala: 1:100.000.

Cucchi, R., 1971. Edades radimétricas y correlación de las metamorfitas de la Precordillera, San Juan- Mendoza, República Argentina. Rev. Asoc. Geol. Argentina 26, 503–515.

Dalla Salda, L.H., Dalziel, I.W.D., Cingolani, C.A., Varela, R., 1992. Did the Taconic Appalachians continue into South America? Geology 20, 1059–1062.

Dalziel, I.W.D., DallaSalda, L.H., Gahagan, L.M., 1994. Paleozoic Laurentia-Gondwana interaction and the origin of the Appalachian–Andean mountain system. Geol. Soc. Am. Bull. 106, 243–252.

Davis, J.S., 1997. The Tectonics of Ancient Plate Margins of the Western Americas. Ph.D. thesis. University of California.

Davis, J., Roeske, S., McClelland, W., Snee, L., 1999. Closing an ocean between the Precordillera terrane and Chilenia: early Devonian ophiolite emplacement and deformation in the southwest Precordillera. In: Ramos, V.A., Keppie, J.D. (Eds.), Laurentia-Gondwana Connections before Pangea, vol. 336. Geological Society of America Special Publication, pp. 115–138.

Davis, J., Roeske, S., McClelland, W., Kay, S.M., 2000. Mafic and ultramafic crustal fragments of the southwestern Precordillera terrane and their bearing on tectonic models of the early Paleozoic in western Argentina. Geology 28 (2), 171–174.

Dias, H., Zanoni de Tonel, M., 1987. La filiación ofiolítica de las rocas ultramáficas de la sierra de Cortaderas (depto. de Las Heras, provincia de Mendoza) y su significación metalogenética en la fijación de pautas de prospección. In: 10° Congreso Geológico Argentino, Actas 1, pp. 61–64.

Dias, H., Zanoni de Tonel, M., 1992. Complejos estratificados ofiolíticos de Cortaderas. In: de Brodtkorb, M.K., Shalamuk, I.B. (Eds.), Primeras Jornadas de Mineralogía, Petrografía y Metalogénesis de Rocas Ultrabásicas, vol. 2. Instituto de Recursos Minerales, Universidad Nacional de La Plata, Publicación, pp. 465–474.

Dilek, Y., Furnes, H., 2011. Ophiolite genesis and global tectonics: geochemical and tectonic fingerprinting of ancient oceanic lithosphere. Geol. Soc. Am. Bull. 123, 387–411.

Donelly, K., Goldstein, S., Langmuir, C., Spiegelman, M., 2004. Origin of enriched ocean ridge basalts and implications for mantle dynamics. Earth Planet Sci. Lett. 226, 347–366.

Fauqué, L.E., Villar, L.M., 2003. Reinterpretación estratigráfica y petrología de la Formación Chuscho, Precordillera de La Rioja. Rev. Asoc. Geol. Argentina 58 (2), 218–232.

Gale, A., Dalton, C., Langmuir, C.H., Su, Y., Schilling, J.G., 2013. The mean composition of ocean ridge basalts. Geochem. Geophys. Geosyst. 14, 489–517.

Gerbi, C., Roeske, S.M., Davis, J.S., 2002. Geology and structural history of the southwestern Precordillera margin, northern Mendoza Province, Argentina. J. South Am. Earth Sci. 14, 821–835.

González-Menéndez, L., Gallastegui, G., Cuesta, A., Heredia, N., Rubio-Ordóñez, A., 2013. Petrogenesis of Early Paleozoic basalts and gabbros in the western Cuyania terrane: constraints on the tectonic setting of the southwestern Gondwana margin (Sierra del Tigre, Andean Argentine Precordillera). Gondwana Res. 24 (1), 359–376.

Haller, M.J., Ramos, V.A., 1984. Las ofiolitas famitinianas (Eopaleozoico) de las provincias de San Juan y Mendoza. In: 9° Congreso Geológico Argentino, Actas 3, pp. 66–83.

Haller, M.J., Ramos, V.A., 1993. Las ofiolitas y otras rocas afines. In: Ramos, V.A. (Ed.), Geología y Recursos Naturales de Mendoza, Relatorio 12° Congreso Geológico Argentino, pp. 31–39.

Hémond, C., Hofmann, A.W., Vlastélic, I., Nauret, F., 2006. Origin of MORB enrichment and relative trace element compatibilities along the Mid-Atlantic Ridge between 10° and 24°N. Geochem. Geophys. Geosyst. 7 (12), 1–22.

Kay, S.M., Ramos, V.A., Kay, R., 1984. Elementos mayoritarios y trazas de las vulcanitas ordovícicas de la Precordillera occidental; basaltos de rift oceánico temprano(?) próximo al margen continental. In: 9° Congreso Geológico Argentino, Actas 2, pp. 48–65.

Kay, S.M., Maksaev, V., Mpodozis, C., Moscoso, R., Nasi, C., 1987. Probing the evolving Andean lithosphere: mid-late Tertiary magmatism in Chile (29° to 30.5°S) over the zone of subhorizontal subduction. J. Geophys. Res. 92, 6173–6189.

Kay, S.M., Orrell, S., Abruzzi, J.M., 1996. Zircon and whole rock Nd–Pb isotopic evidence for a Grenville age and Laurentia origin for the basament of the Precordilleran terrane in Argentina. Geol. Soc. Am. South-Central Sec. Abs. Prog. 28 (1), 21–22.

Kay, S.M., Boucakis, K.A., Porch, K., Davis, J.S., Roeske, S.M., Ramos, V.A., 2005. E-MORBlike mafic magmatic rocks on the western border of the Cuyania terrane, Argentina. In: Pankhurst, R.J., Veiga, G.D. (Eds.), Gondwana 12 "Geological and Biological Heritage of Gondwana", p. 216.

Leveratto, M.A., 1968. Geología del oeste de Ullum-Zonda, borde oriental de la Precordillera de San Juan. Rev. Asoc. Geol. Argentina 23 (2), 129–157.

Loeske, W.P., 1993. La Precordillera del oeste argentino: una cuenca de *back arc* en el paleozoico. In: 12° Congreso Geológico Argentino, Actas 1, pp. 5–13.

McDonough, W.F., Sun, S.-S., 1995. The composition of the Earth. Chem. Geol. 120, 223–253.

Moyen, J.F., 2009. High Sr/Y and La/Yb ratios: the meaning of the "adakitic signature". Lithos 112 (3–4), 556–574.

Niu, Y., Regelous, M., Wendt, I.J., Batiza, R., O'Hara, M.J., 2002. Geochemistry of near-EPR seamounts: importance of source vs. process and the origin of enriched mantle component. Earth Planet Sci. Lett. 199 (3–4), 327–345.

Ortiz, A., Zambrano, J.J., 1981. La provincia geológica Precordillera oriental. In: 8° Congreso Geológico Argentino, Actas 3, pp. 59–74.

Quartino, B., Zardini, R., Amos, A., 1971. Estudio y exploración geológica de la región Barreal- Calingasta, provincia de San Juan, República Argentina. Monografía N° 1. Asociación Geológica Argentina, Buenos Aires.

Ramos, V.A., Jordan, T.E., Allmendinger, R.W., Mpodozis, C., Kay, S.M., 1984. Chilenia: un terreno alóctono en la evolución de los Andes centrales. In: 9° Congreso Geológico Argentino, Actas 2, pp. 84–106.

Ramos, V.A., Jordan, T.E., Allmendinger, R.W., Mpodozis, C., Kay, S.M., Cortés, M., Palma, M., 1986. Paleozoic terranes of the central Argentine–Chilean Andes. Tectonics 5, 855–880.

Rapela, C.W., Pankhurst, R.J., Casquet, C., Baldo, E., Galindo, C., Fanning, C.M., Dahlquist, J.M., 2010. The Western Sierras Pampeanas: protracted Grenville-age history (1330–1030 Ma) of intra-oceanic arcs, subduction–accretion at continental-edge and AMCG intraplate magmatism. J. South Am. Earth Sci. 29, 105–127.

Robinson, D., Bevins, R.E., Rubinstein, N., 2005. Subgreenschist facies metamorphism of metabasites from the Precordillera terrane of western Argentina; constraints on the later stages of accretion onto Gondwana. Eur. J. Mineral. 17, 441–452.

Rubinstein, N., Bevins, R., Robinson, D., Morello, O., 1998. Very low metamorphism in the Alcaparrosa formation, western Precordillera, Argentina. In: 10° Congreso Latinoamericano de Geologiay 6° Congreso Nacional de Geología Económica, Actas 2, pp. 326–329.

Schilling, J.G., 1973. Iceland mantle plume: geochemical study of the Reykjanes Ridge. Nature 242, 565–571.

Sun, S.-s., McDonough, W.F., 1989. Chemical and isotopic systematics of oceanic basalts: implications for mantle composition and processes. Magmatism in the Ocean Basins. Geol. Soc. Lon. Spec. Publ. 42, 313–345.
Taylor, S., McLennan, S., 1985. The Continental Crust: its Composition and Evolution. An Examination of the Geochemical Record Preserved in Sedimentary Rocks. Blackwell, Oxford.
Thomas, W.A., Astini, R.A., 2003. Ordovician accretion of the Argentine Precordillera terrane to Gondwana: a review. J. South Am. Earth Sci. 16, 67–79.
Thomas, W.A., Tucker, R.D., Astini, R.A., Denison, R.E., 2012. Ages of pre-rift basement and synrift rocks along the conjugate rift and transform margins of the Argentine Precordillera and Laurentia. Geosphere 8 (6), 1–18.
Ulrich, M., Hémond, C., Nonnotte, P., Jochum, K.P., 2012. OIB/seamount recycling as a possible process for E-MORB genesis. Geochem. Geophys. Geosyst. 13 (6). http://dx.doi.org/10.1029/2012GC004078. Article numberQ0AC19.
von Gosen, W., 1997. Early Paleozoic and Andrean structural evolution in the Rio Jachal section of the Argentine Precordillera. J. South Am. Earth Sci. 10, 361–388.
White, W.M., Hofmann, A.W., 1982. Sr and Nd isotope geochemistry of oceanic basalts and mantle evolution. Nature 291, 821–825.
Willner, A.P., Gerdes, A., Massonne, H.-J., Schmidt, A., Sudo, M., Thomson, S.N., Vujovich, G., 2011. The geodynamics of collision of a microplate (Chilenia) in Devonian times deduced by the pressure-temperature-time evolution within part of a collisional belt (Guarguaraz Complex, W-Argentina). Contribut. Mineral. Petrol. 162, 303–327.
Winchester, J.A., Floyd, P.A., 1976. Geochemical magma type discrimination: application to altered and metamorphosed basic igneous rocks. Earth Planet Sci. Lett. 28 (3), 459–469.
Winchester, J.A., Floyd, P.A., 1977. Geochemical discrimination of different magma series and their differentiation products using immobile elements. Chem. Geol. 20, 325–343.
Wood, D.A., Joron, J.L., Treuil, M., 1979. A reappraisal of the use of trace elements to classify and discriminate between magma series erupted in different tectonic settings. Earth Planet Sci. Lett. 45 (2), 326–336.
Zindler, A., Hart, S., 1986. Chemical geodynamics. Annu. Rev. Earth Planet Sci. 14, 493–571.